Journal of Nanoparticle Research **4:** 21–41, 2002.

Review paper

Mixing and characterization of nanosized powders: An assessment of different techniques

Dongguang Wei, Rajesh Dave and Robert Pfeffer*
New Jersey Center for Engineered Particulates, New Jersey Institute of Technology, Newark, NJ 07102, USA;
**Author for correspondence (Tel.: +1-973-642-7496; Fax: +1-973-642-7088; E-mail: pfeffer@njit.edu)*

Received 2 July 2001; accepted in revised form 27 November 2001

Key words: mixing, characterization, nanoparticles, dry particle processing, RESS

Abstract

The objective of this paper was to gain an understanding of the mixing and characterization of nanosized powders. Three different nanosized material systems were selected based on their physical and chemical properties. Mixing experiments of the selected nanopowders were performed using a variety of environmentally friendly dry powder processing devices and the rapid expansion of supercritical CO_2 suspensions (RESS process) and compared with solvent-based methods coupled with ultrasonic agitation. A number of imaging techniques, including FESEM, AFM, TEM, EELS and EDS were used to characterize the degree of mixing or homogeneity of the mixtures obtained.

The results indicate that only some of the imaging techniques are capable of determining the quality of nanoparticle mixing, depending on the physical and chemical properties of the nanopowders. For example, field emission scanning electron microscope (FESEM) is suitable for characterizing powder mixtures having a distinct difference in particle shape, or with a large difference in atomic number of the metallic element of the two constituents. Only electron energy loss spectroscopy (EELS) was able to fully characterize nanopowder mixtures of SiO_2 and TiO_2 at the nanoscale. Energy dispersive X-ray spectroscopy (EDS) provided information on mixing quality, but only on a scale of about 1 μm. The results also show that solvent-based mixing methods coupled with ultrasonic agitation, and RESS generally perform better than dry powder processing systems, with the exception of the hybridizer, in generating a homogeneous mixture.

Introduction

This paper addresses the subject of mixing of ultrafine particles and the available methods for characterizing the degree of mixing of nanoparticles to form nanocomposites. This is a relatively new area of research, which has a high potential for many commercial applications, both industrial and military. However, very few papers are found in the literature regarding the mixing of highly cohesive powders, let alone the mixing of nanoparticles. This is due to the fact that most traditional powder technology applications do not deal with powders smaller than about 20 μm. Thus, the vast literature available in the area of mixing and characterization of non-cohesive powders has little to offer, since the behavior of nanoparticles is very different from the behavior of conventional powder materials.

Nanocomposites

It is expected that the next generation of high-performance structural materials and coatings will routinely employ nanoparticles and nanocomposites due to their attractive qualities such as wear resistance, corrosion resistance, mechanical strength and hardness. Nanoparticles and nanocomposites are also being used as high-performance catalysts, and as advanced energetic, electronic, photonic, magnetic and biomedical materials. All of these applications require an

understanding of the handling and mixing properties of nanostructured materials.

The unique properties of nanoparticles arise from their size reduction. When a particle is reduced down to the nanosize range (usually defined as 1–100 nm), a much larger surface area per unit volume is achieved, and even more importantly, a dramatically increased percentage of molecules or atoms are found to be present on its surface. At the point where the interaction length scales of physical, chemical and biological phenomena become comparable to the size of the particle, crystal or grain structure, new properties and phenomena emerge (Roco, 1999; Siegel, 1999). These unique properties of nanostructured materials are extremely important, for example, in developing new and advanced catalysts (Trudeau & Ying, 1996; Moser et al., 1996; Ying, 1997; Zhang et al., 1998; Fokema et al., 2000).

Furthermore, when two or more phases are mixed together to make a nanocomposite, a combination of properties can be obtained, which are not available in any of the individual components, since at this scale, macroscopic material properties are strongly influenced by atomic or molecular interactions. Since the building blocks of a nanocomposite are of nanoscale, many interfaces exist between the two intermixed solid phases and the special properties of a nanocomposite arise from phase interactions at these interfaces (Ajayan, 1995; Gross et al., 1996; Ajayan et al., 1997; Carter et al., 1997; Maser et al., 1997; Imanaka et al., 2000). Thus, the ability to prepare well-mixed nanocomposites is extremely important.

Two different approaches, spray forming and powder processing (Kear & Skandan, 1997; 1999) have been proposed for the preparation of nanocomposites. Spray forming combines nanoparticle synthesis, heating and consolidation into one single operation. In powder processing, nanoparticles of the desired materials are first synthesized by some convenient chemical or physical methods, and then structurally assembled via some steps that may include mixing, and finally consolidated through sintering or some other methods.

Dry particle mixing

Mixing of solid particles has been one of the basic operations performed by man for thousands of years. For example, the mixing of the ingredients for gunpowder can be dated as early as 700 BC. Dry particle mixing is an essential and very important unit operation in industries dealing with powders and bulk solids, including ceramics, plastics, detergents, foods, pharmaceuticals, advanced materials, etc. and has received extensive study during the past decades. However, Williams (1990) says, 'Although the mixing of particulate solids is one of the oldest and most important operations in the process industries, it is one of the least well understood'.

A number of recently published reviews (Fan et al., 1990; Williams, 1990; Poux et al., 1991; Parent et al., 1993; Ottino & Khakhar, 1997) and monographs (Kaye, 1997; Rhodes, 1998; Myers, 1999; Weinekotter & Gericke, 2000) on this subject appear in the literature and the various mechanisms of mixing of solid particles are discussed. Different types of mixers, such as tumbling mixers, convective mixers, fluidized bed mixers, high-shear mixers, including media mills and hammer mills, are also described in detail (see Kaye (1997) for a comprehensive review and discussion). However, most of the existing literature deals primarily with either free-flowing particle systems or cohesive powder systems of a relatively large size, for example, mean particle sizes greater than 10–20 μm. Only limited research is concerned with mixing of cohesive powders (Kaye, 1997; Rhodes, 1998) or particles smaller than 1 μm (Parent et al., 1993; Carter et al., 1997; Gulliver et al., 1997).

Mixing evaluation and sampling

Many different methods have been described in the literature for evaluating the homogeneity of a mixture of different powder particles (Fan et al., 1990; Kaye, 1997; Rhodes, 1998; Weinekotter & Gericke, 2000). One method involves evaluating the mixture by its end-use properties (Danckwerts, 1953). For example, if a well-mixed nanosized metal and nanosized metal oxide powder becomes energetic, then the degree of mixing can be determined by how well the mixture explodes. Although this is not a very accurate or direct method to characterize mixing, it is often employed in industry.

More often, the degree of mixing is determined by analyzing images of particle arrays within a sample of the mixture using microscopy, photography and/or video tools. The images of the two-component mixture of particles may be distinguishable by a distinct particle shape, color, or some other surface characteristic (Parent et al., 1993; Gulliver et al., 1997; Kaye, 1997; Hill et al., 1999). In some cases, a tracer is used for examining the degree of mixing (Wang & Fan, 1976; Brone et al., 1998; Brone & Muzzio, 2000).

For mixtures of nanoparticles, obtaining a reliable assessment of particle positions in an array and distinguishing between the different species is very difficult. From a molecular viewpoint, a powder mixture can never achieve perfect homogeneity, and thus the degree of mixing becomes a relative concept. Therefore, an evaluation of mixing at the scale of individual nanoparticles is nearly impossible and probably unnecessary. However, the degree of mixing at different length scales may need to be evaluated which further complicates the issue, since the sample size, number of measurements, and the method of obtaining the samples, all become very important. Most current indices of the degree of mixing are based on the measurement of sample variances. Fan et al. have reviewed and analyzed over 30 different indices of the degree of mixing proposed by various researchers and some additional indices have been proposed since then (Fan et al., 1990). All of these require extensive sampling, especially when evaluating mixtures of nanoparticles.

The sampling technique used is also an important issue in the characterization of powder mixing. For example, the widely used theft-probe sampling method can yield non-representative samples (Thiel & Stephenson, 1982). Therefore, statistical analysis is usually applied to the measurement data (Harnby, 1978; Rhodes, 1998; Weinekotter & Gericke, 2000) to obtain more reliable results, along with a larger sample size, that is, a larger number of measurements.

Mixing and characterization of nanoparticles

In order to determine the feasibility of a mixing process for highly cohesive nanoparticles, it is necessary to estimate the forces generated during mixing and show that these forces are larger than the cohesive or adhesive forces acting on the powder particles. Interparticle forces can be classified into two groups: forces such as van der Waals, electrostatic and magnetic attraction, mechanical interlocking and chemical, that is, those which do not require material bridges, and forces due to solid bridges, capillary bonding forces and immobile liquid bridges, that is, those where a material bridge is present. In general, at low humidity, the first group is important, and at high humidity, the second becomes more important. Consequently, for dry particle mixing, the cohesive and adhesive forces acting between particles depend on molecular forces, and their importance decreases with increasing particle size.

Body forces (gravity) are proportional to the cube of the particle diameter, while van der Waals forces are proportional to the particle diameter. Thus, for relatively large particles (greater than 10–20 μm), the interparticle forces are small compared to the particle weight, and their role in mixing can be neglected and the effectiveness of a dry mixing process can be analyzed in terms of the macroscopic forces applied. Specifically, it can be shown that these powders can be mixed provided the applied macroscopic forces, that is, the shear and extensional/compressive stresses are large enough to break any loosely formed aggregates. In most cases, this can be achieved by simply agitating the powder, and the only concern in mixing of these powders is the mixing efficiency. The overall motion of particles must be appropriate for obtaining efficient mixing and can be quantified in terms of the spatial distribution of the particle trajectories.

For dry particle mixing of powders less than 1 μm in size, on the other hand, an understanding of the macroscopic motion and forces alone is not sufficient to determine whether the mixing will take place at a scale comparable to the effective diameter of an individual particle (Verkhovluyk, 1993; Kwak, 1994). Clearly, if the external stresses generated are not large enough to break up the aggregates that have been created due to van der Waals, Coulombic and other cohesive forces, mixing will not occur at scales smaller than the size of the aggregates. Another complication is that when fine powder is sheared or agitated, slip planes form, which relieve the stresses, leaving the bulk of the powder with no relative motion or shear. The macroscopic mixing process, therefore, must be designed to ensure that the shear flow is generated at the length scales at which mixing is desired. In other words, micro-shear or high-intensity impacts are required. The process of mixing must involve both a break up of the agglomerated nanoparticles and a dispersion of individual or small clusters of nanoparticles of one phase into the other.

At present, mixing of nanoparticles can be achieved by simply suspending the two different powders (with agitation) in an organic liquid. This wet process appears to be the only technique that is widely used, although it requires drying of the mixture and is environmentally unfriendly due to VOC emissions. However, it is also used here for baseline performance comparison with other methods.

As an alternative to the wet mixing process, we propose using environmentally benign dry particle mixing and/or mixing of nanoparticles using supercritical

CO_2. In dry particle mixing, a number of innovative mechanical devices are utilized. Mixing with supercritical CO_2 uses a modified rapid expansion of supercritical suspension (RESS) process.

Reports in the Japanese literature, and subsequent research at NJIT (see Pfeffer et al. (2001) for a comprehensive review), suggested that the various equipment available for dry powder surface modification and dry coating of micron-sized host particles by submicron-sized guest particles could also be used to achieve nanomixing. These devices employ special purpose, high-intensity mechanical processing to deagglomerate the fine, highly cohesive guest powders. Four different dry coating devices are considered. Each device is unique in its 'deagglomeration' mechanism; for example, it can provide micro-shear as well as intense local shear fluctuations, high-intensity impacts, and/or a substantial increase in the body force of the particles by subjecting them to high centrifugal accelerations.

In a recent paper, Endo et al. (1997) showed that a rapid pressure drop in a gas stream of powder agglomerates can lead to deagglomeration. The success of this technique depends on the characteristic time for pressure release within the pores of the agglomerates as compared to the time in which the agglomerate travels from a zone of high pressure to low (nearly atmospheric) pressure. If the latter is smaller, then the agglomerate will 'explode' due to a large pressure gradient and deagglomeration should occur. In the RESS process approach for nanomixing, this idea is exploited along with the advantages of mixing in a low viscosity, high diffusivity and variable density fluid such as supercritical CO_2.

The characterization of nanoparticle mixtures requires high-resolution instruments that can image nanosized particles. A variety of electron microscopy instruments along with elemental analysis (energy dispersive X-ray spectroscopy (EDS)) can be used. Another approach involves using atomic force microscopy (AFM). The AFM can provide a topographical map of the sample surface with a resolution down to a few nanometers. If the two different nanoparticle materials have distinctly different morphology, AFM imaging can be used to tell them apart. An AFM equipped with phase imaging capability (sensitive to variations in material properties such as adhesion or viscoelasticity), can also record the phase map along with the surface topography, which makes it a good choice for the characterization of mixing of nanoparticles of similar size and morphology.

Experimental procedure

The study employed three different material systems. The selection of the material systems was based on their physical and chemical properties for the purpose of evaluating the performance of various mixing methods and devices and to demonstrate different characterization methods. As discussed above, mixing of the nanopowders was carried out using solvent-based, dry powder and supercritical processing methods. The physical characterization of the resultant mixtures was conducted using a number of different commercially available imaging and microanalysis instruments.

Material systems

The three material systems selected to perform mixing experiments in this study were: (1) MS-1: nanosized tungsten metal powder and nanosized molybdenum trioxide powder, (2) MS-2: micron-sized tungsten metal powder and sub-micron-sized titania powder, and (3) MS-3: nanosized silica and titania powders. The physical properties of these materials are listed in Table 1. The mass (grams) of each of the constituents in all three of the material systems were chosen so that there are approximately equal numbers of particles of each of the two constituents.

Table 1. Summary of the physical properties of the materials used in the mixing study

Material system	Powder	Nominal particle size	True density (g/cm^3)	Bulk density (g/cm^3)	Source
MS-1	W (1)	100 nm	19.3	4.15	Argonide, Inc.
	MoO_3	20 nm	4.70	0.24	Picatinny Arsenal
MS-2	W (2)	1.0 μm	19.3	3.54	Micron Metal, Inc.
	TiO_2 (1)	300 nm	4.26	0.88	Micron Metal, Inc.
MS-3	TiO_2 (2)	25 nm	4.26	0.18	Degussa, P25
	SiO_2	16 nm	2.20	0.05	Degussa, R972

Mixing tests

The mixing of powders was carried out in three different ways: (1) solvent-based methods, (2) dry powder processing methods, and (3) RESS.

Solvent-based methods
The two component powders were weighed and suspended in a solvent in a beaker. The beaker was then placed in an ultrasonic bath of water. After a certain time of ultrasonic agitation, the colloidal suspension was dried and the mixture was collected for characterization. The ultrasonic bath employed in this experiment was an FS-30 ultrasonic cleaner (Fischer Scientific) with a power of 100 W at a fixed frequency of 44–48 kHz. Specifically, for the nanosized silica and titania system (MS-3), 3.6 g of titania (25 nm, Degussa P25) and 1.4 g of silica (16 nm, Degussa R972) were weighed and then suspended in 60 ml ethanol (CP, Fischer Scientific) or 60 ml hexane (CP, Fischer Scientific). The suspension was then ultrasonically agitated for either 5 or 30 min. After ultrasonication, the suspension was dried overnight in an oven at 383 K. The dried mixture was then collected in a sealed vial for characterization. For system MS-1, the mixing of nanosized W (100 nm, Argonide) and MoO_3 (20 nm, Picatinny Arsenal), 5 g of W and 1 g of MoO_3 were used. All other procedures were the same as described above for MS-3. The system MS-2 was not considered for wet mixing.

Dry powder processing methods
As mentioned above, four different mechanical devices were used for dry mixing of nanopowders. These devices, although differing in their manner of supplying the necessary mechanical forces, are all designed to promote deagglomeration of cohesive nanopowders so as to facilitate the dispersion of particles of one component into the other to achieve a high degree of mixing.

Magnetically assisted impaction mixing. This device was developed at our laboratory based on a system used for dry particle coating (Singh et al., 1997; Hendrickson & Abbott, 1999; Ramlakhan et al., 2000; Pfeffer et al., 2001). The two component powders to be mixed, along with larger magnetic particles (which are coated with polyurethane) are placed in a non-metallic container. The container is then subjected to an oscillating magnetic field causing the magnetic particles to translate and spin violently and undergo collisions with the walls and the other particles. As a result, the whole system appears fluidized, although no fluidizing gas is present. Mixing in this device appears to be due to the micro-shear created by individually spinning magnetic particles and subsequent multiple collisions that take place between the powder agglomerates.

In the mixing of MS-3 (nanosized silica and titania), 3.6 g of titania and 1.4 g of silica were weighed and charged into the container of volume of 200 ml. Fifteen grams of magnetic particles (with a size range from 1.7 to 2.4 mm) were magnetized and then mixed with the powders in the container and the oscillating magnetic field turned on. After 30 min of processing, the mixture was discharged and sieved to remove the magnetic particles. The powder mixture was collected for characterization and the magnetic particles were cleaned for the next experiment. For mixing of MS-2 [W (1 μm) and TiO_2 (300 nm)], 19 g W and 1 g TiO_2 were used. The procedure and conditions used were the same as for the mixing of MS-3.

Hybridization system. The hybridization system (HYB) from Nara Machinery of Japan has been used for making ordered mixtures, and for dry coating and encapsulation of host particles by guest particles (Ishizaka et al., 1993). The hybridizer consists of a cylindrical chamber with a high-speed rotor (spinning at up to 16,000 rpm) with six blades connected to a powder recirculation system (Koishi et al., 1987; Honda et al., 1988; 1994; Ishizaka et al., 1993; Pfeffer et al., 2001). Due to high centrifugal forces and relatively low powder loading, particles move violently within the system. They undergo many collisions with the rotating blades, and with one another, allowing for the break up of agglomerates and mixing. Mixing in this device appears to be due to the high-intensity collisions and very large centrifugal forces acting on the nanopowder agglomerates.

In the mixing experiment, 10 g of MS-3 (7.2 g titania and 2.8 g silica) was charged into the chamber of the system (model NS-01) and dry air at a pressure of 5 atm was introduced. The rotor speed was varied from 5000 to 16,000 rpm. The mixing experiment was run for only a few minutes (2–10 min). Material systems MS-1 and MS-2 were not used in the hybridizer.

Mechanofusion. Mechanofusion (MF) is another dry powder coating system and was originally developed by Hosokawa Micron Corp. for ultrafine material grinding and powder alloying (Yokoyama et al., 1987; Tanno et al., 1994; Chen et al., 1997; Pfeffer et al., 2001).

This device has a cylindrical drum that rotates at high speed (up to 3000 rpm), while a stationary internal arm, which has a cylindrical surface at the end, creates intense shear and compressive forces on the powder mixture pinned between the arm and the cylindrical drum. There is also a stationary scraper, which prevents powder from caking against the wall. Mixing in this device appears to be due to the high-intensity compressive and shear forces and high level of centrifugal forces that the agglomerates experience.

Since this device needs at least a volume of 80–100 ml of material to achieve a good processing result, only material systems MS-2 and MS-3 were used to conduct the mixing experiments. Specifically, 120 g W and 6 g TiO_2 were used for mixing MS-2, and 28.8 g titania and 11.6 g silica were used for mixing MS-3 in the MF.

Micros. The Micros (MIC) superfine mill was developed by Nara Machinery of Japan for grinding powder materials in a liquid media. It has also been used for creating mechanochemical reactions for various ceramic powders (Hamada & Senna, 1995; 1996). The lab scale (MIC-0) device consists of a vessel (300 ml effective inner volume) with a cooling jacket, a rotating main shaft and six sub-shafts interlocked with the main shaft. A number of loosely stacked rings, serving as milling media, are centered on each sub-shaft. The particles are held between the revolving set of rings on the sub-shaft and the cylindrical wall surface and are subjected to compression forces created by the centrifugal action of the rings and friction created by individual rotating rings. Each ring in a set of rings can move independently of each other adjusting to the size of the particles/agglomerates between the rings and the wall. This process produces pulverization, dispersion and intense mixing of particles. It has also been found to grind powders down to sub-micron sizes. Hence it appears to be capable of breaking down agglomerates of nanoparticles and should be effective as a nanopowder mixer.

In this study the device was used as a dry mixer to avoid the problem of solvent removal. Only material MS-3 (7.2 g titania and 2.8 g silica) was processed in this device (for 5 min at 1200 rpm).

Rapid expansion of supercritical suspensions

Rapid expansion of supercritical solutions and/or suspensions has been employed for particle formation of organic substances, especially polymers and polymer–drug composites (Tom & Debenedetti, 1991; Reverchon et al., 1993; Tom et al., 1993; Alessi et al., 1996; Turk, 1999; York, 1999). The RESS process has been developed to exploit the advantages of supercritical fluids, such as increased solubility of solutes as compared to a gas, and higher diffusivity and very low surface tension and viscosity as compared to a liquid, pressure-dependent density, etc. For conducting powder mixing studies, a two-stage system was built (see Figure 1) and carbon dioxide was used as the supercritical medium.

The MS-3 powder (3.6 g titania and 1.4 g silica) was charged into the first-stage vessel (300 ml) and was heated and pressurized with CO_2 using a heating jacket and a supercritical CO_2 pump to the desired conditions in the supercritical regime. A stirring device was also incorporated in the first-stage vessel. After a certain time of stirring at 1000–2000 rpm under steady-state supercritical conditions, the suspension was released through a nozzle into a second-stage vessel (2000 ml), the CO_2 gas was vented through a filter and the powder mixture was collected from the second-stage vessel.

Characterization of nanoparticle mixtures

A number of different imaging and microanalysis techniques have been used for characterizing the mixtures produced by the experiments. It should be noted that since the nanopowders are highly cohesive, we believe that none of the sample preparation techniques described below should have any effect on the quality of mixing. Furthermore, a number of samples were prepared by hand-mixing, that is, shaking the two powders in a bottle. These samples, when inspected under a high-resolution transmission electron microscope (TEM), showed that the samples were essentially unmixed.

Field emission scanning electron microscope

After each mixing experiment, the powder mixture was first examined using either a LEO 982 Digital Field Emission Electron Scanning Microscope or a JEOL JSM-6700F Field Emission Electron Scanning Microscope. The field emission scanning electron microscope (FESEM) was operated at accelerating voltages from 10 to 20 kV in either secondary electron detector (SE) mode or backscattered electron detector (BSE) mode depending on the sample properties. The working distance varied from 3 to 8 mm for SE mode; 8 mm was preferred for BSE mode. The

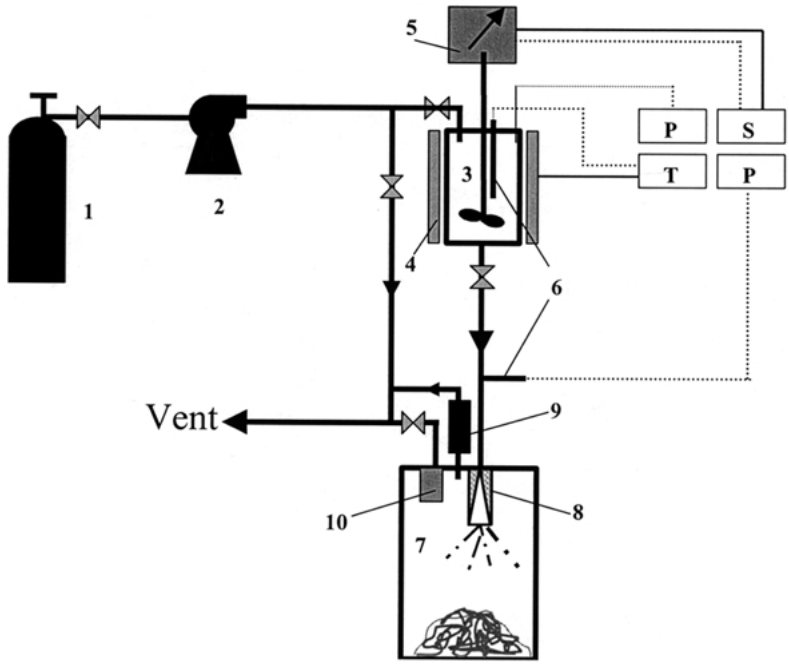

Figure 1. Schematic diagram of the experimental system used for RESS. CO_2 cylinder (1), supercritical CO_2 pump (2), reactor (3), heating jacket (4), speed adjustable stirring system (5), thermocouple (6), receiving tank (7), spray nozzle (8), release valve (9) and filter (10) are shown.

powder mixture was put under the SEM detector either as loosely scattered powder or as a pressed wafer. The wafer, with a diameter of 15 mm and a thickness of about 1 mm, was prepared by compressing the mixed powder using a lab press without any additives at constant pressure for a constant time period. No measurable differences in the degree of mixing between the loosely scattered powder and the wafer (of the same sample) could be observed using EDS spot analysis (see below). Therefore, it was assumed that pressing the powder into a wafer did not affect the degree of mixing of the processed sample.

Transmission electron microscope

The powder mixtures were also investigated using a 200 kV Phillips CM20 Transmission Electron Microscope equipped with a Schottky field-emission source. The samples were investigated in loosely scattered form.

Electron energy loss spectroscopy

A 100 kV VG Microscopes HB501 UX Scanning Transmission Electron Microscope equipped with electron energy loss spectroscopy (EELS) (available at Oak Ridge National Laboratory) and a LEO 922 Omega Filter TEM equipped with EELS (available at the LEO Applications Laboratory) were both used to examine a few samples of the nanoparticle powder mixture, MS-3. The powder mixture samples were investigated under the microscope detector in loosely scattered form. EELS imaging technique employs a unique design to achieve both angle selection and energy selection of elastically and inelastically scattered electrons. By assigning an 'energy window' in an energy loss spectrum region, EELS is able to image a specific element in a sample while a global image can be recorded simultaneously under zero energy loss conditions (as in a conventional TEM). Therefore, a comparison between the global image and the elemental images can indicate the distribution of different materials.

Atomic force microscope

The morphologies of some of the mixed samples were examined using a Digital Instruments Nanoscope IIIa Atomic Force Microscope. The AFM was operated in tapping mode and all scans were performed at ambient

conditions (constant temperature) on the pressed wafer samples which were first blown with a compressed inert gas to remove particles loosely attached to the sample surface. In addition to surface morphology, the phase imaging mode of the AFM can, in principle, be used to detect variations in composition, adhesion, friction, viscoelasticity, and other properties of the mixture.

Energy dispersive X-ray spectroscopy

In order to analyze the chemical composition of the surface of a mixture, EDS was employed. The spectra were collected using a LEO Field Emission Scanning Electron Microscope equipped with an Oxford UTW X-ray detector. The spectrum was obtained under an accelerating voltage of 15 keV and a working distance of 14 mm. To assure a consistent analysis, all of the samples used in these tests were carefully compressed into a wafer of a diameter of 15 mm about 1 mm thick (as discussed above) under constant pressure (20,000 lb/in^2) for the same time period.

Results and discussion

While all three material systems were used to determine the performance of the different mixing methods/devices and to examine the applicability of different characterization techniques, the major emphasis was on the mixing of system MS-3 since this was the most challenging, as both components were of primary particle size of 25 nm or less.

MS-1: Nanosized W and MoO_3

The two powders were mixed in hexane under ultrasonic agitation. The dried mixture was collected as a thin cake and directly analyzed using a LEO 982 FESEM (SE detector). The SEM photographs of the mixture of W and MoO_3 are shown in Figure 2 at different magnifications. Two types of particles having very distinct shape characteristics, spherical and crystalline,

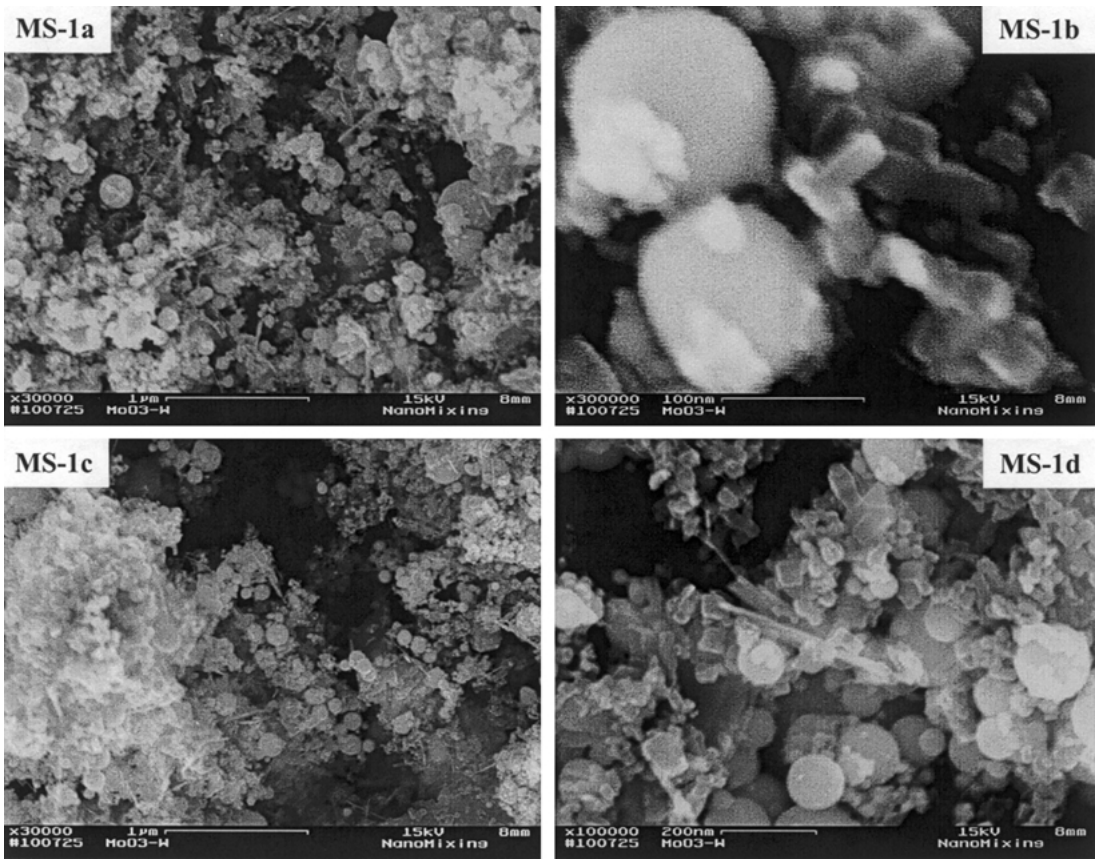

Figure 2. SEM micrographs of MS-1 mixture mixed in hexane for 30 min under ultrasonic agitation.

can be seen. By EDS analysis, it was identified that the spherical particles are W metal, and the crystalline particles (both cubic and needle-like) are MoO_3. The typical particle sizes for both components (W and MoO_3) are close to their nominal diameters although a wide size distribution for both is obvious. W particles can be found either next to MoO_3 particles or within the agglomerates of MoO_3 particles at different length scales, indicating that a homogeneous mixture (to a certain extent) was obtained. It is seen that individual clusters of each component are still present especially at high magnifications. This might be due to the existence of strong forces between the primary particles, that is, a chemical bonding formed during their production (Pierre, 1998), and also indicates that ultrasonic agitation could not break up all of the agglomerates of MoO_3.

The most important observation that can be made from these images is that since the two powder constituents differ distinctly in particle shape, the high-resolution FESEM used in this study is capable of characterizing the mixing at this scale, albeit in a qualitative manner. A sophisticated image analysis procedure is required to derive any quantitative information.

MS-2: Micron-sized W and sub-micron-sized TiO_2

For powders that do not possess very different particle shape characteristics, the analysis of SEM images is much more difficult. The material system MS-2 was designed to demonstrate characterization using the BSE detector. The MS-2 system consists of micron-sized W metal powder and sub-micron-sized TiO_2 powder (see Table 1). These two powders were mixed using two dry mixing devices, magnetically assisted impaction mixing (MAIM) and MF. The samples in loosely scattered form were examined with a LEO 982 FESEM (using both the SE and the BSE detectors). Figures 3 and 4 show some typical SEM photographs of the mixed samples at different magnification processed by MAIM and MF, respectively.

The left-hand side images in Figures 3 and 4 were obtained using the SE detector, while the right-hand

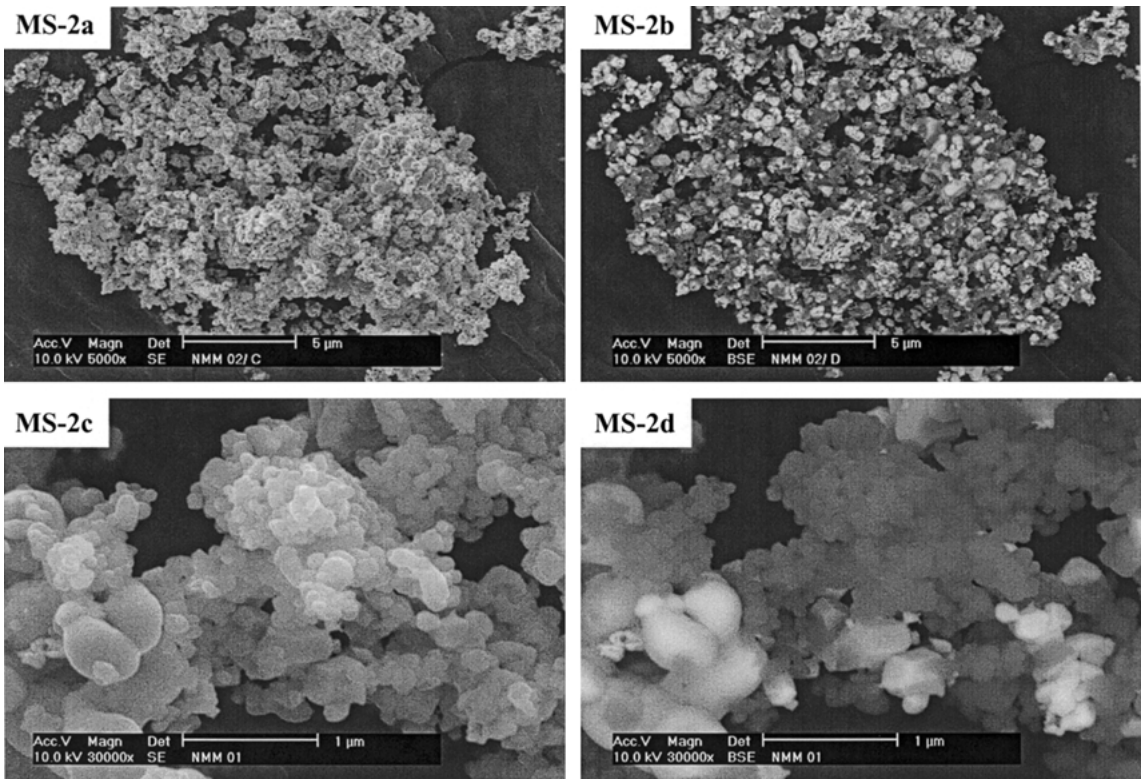

Figure 3. SEM micrographs of MS-2 mixture processed using MAIM: MS-2a and MS-2c are SE images, MS-2b and MS-2d are BSE images of MS-2a and MS-2c, respectively.

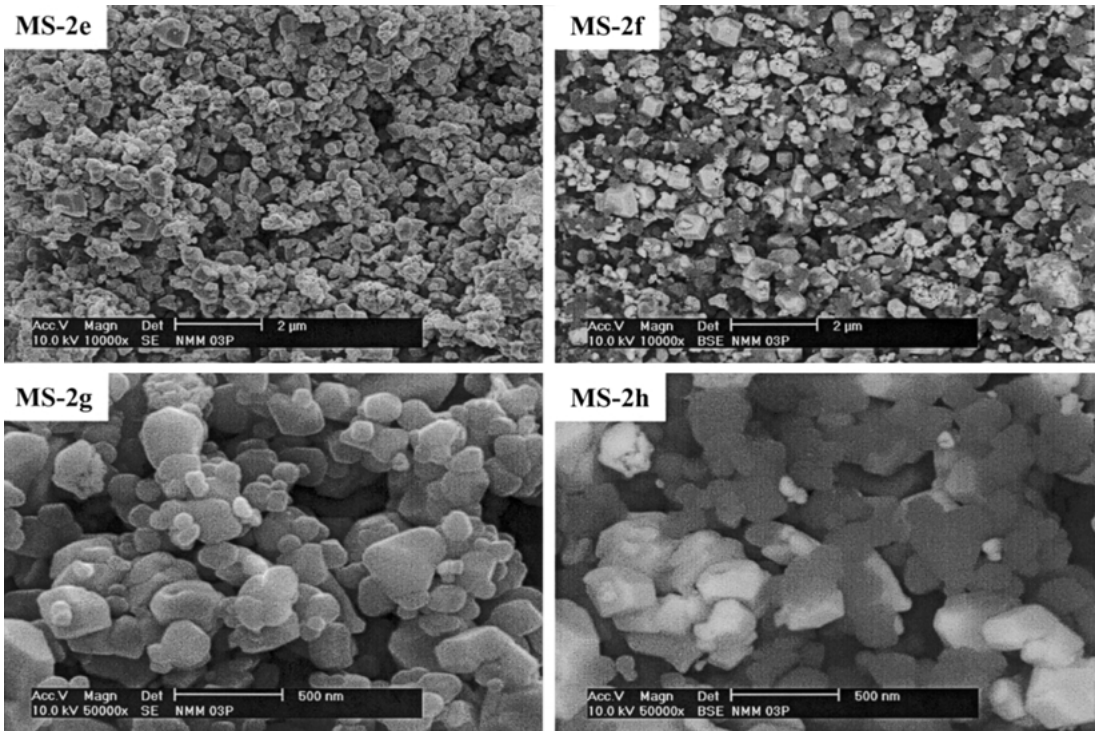

Figure 4. SEM micrographs of MS-2 mixture processed using MF: MS-2e and MS-2g are SE images, MS-2f and MS-2h are BSE images of MS-2e and MS-2g, respectively.

side images were obtained using the BSE detector. In images MS-2b and 2d, two types of particles are seen: bright and dark. It was determined by EDS that the bright particles are W metal, and the dark particles are TiO_2. Comparing MS-2a, -2c, -2e and -2g with MS-2b, -2d, -2f and -2h in Figures 3 and 4, shows that the SE detector only provides information about particle morphologies, whereas the BSE detector distinguishes particles of different chemical composition (i.e., Z-contrast or contrast due to atomic number difference). Thus the BSE detector can be used for characterizing powder mixtures when the component particles do not necessarily possess different shape characteristics (such as MS-1). However, this is not always possible since the difference in the gray scale of the particles seen on the BSE images depends on the difference in atomic number (Z) and the sensitivity of the BSE detector employed. The larger the difference in atomic number, the better the contrast that is obtained on BSE images (Goldstein et al., 1992).

From Figure 3 (MS-2b) and Figure 4 (MS-2f), it appears that both dry mixing devices produced a reasonable homogeneity of mixing. However, if Figure 3 (MS-2d) is compared with Figure 4 (MS-2h), by taking into account the difference in the magnification of the two images (30k for MS-2d and 50k for MS-2h), it is qualitatively observed that MF has performed better than MAIM in terms of particle mixing, since larger agglomerates of both TiO_2 and W are seen in MS-2d. This is not entirely surprising since MF provides much higher forces and collision energy between particles than the comparatively mild fluidization of the powders caused by the random motion of the magnetic particles in MAIM (Honda et al., 1994; Singh et al., 1997). However, it is apparent that agglomerates of various sizes are present in both images, MS-2d and MS-2h, implying that the breakup of agglomerates of fine powders is an extremely difficult process.

Once again, these series of images show that unless a sophisticated image analysis procedure is used, SEM imaging only gives a qualitative indication of the mixing quality.

MS-3: Nanosized SiO_2 and TiO_2

The mixing of particles of size range between a few nanometers and one hundred nanometers is extremely difficult since the interparticle forces are much higher

than those between particles of size range greater than 1 μm. Nanosized SiO_2 (16 nm) and TiO_2 (25 nm) were used as the model system (MS-3) to perform mixing and characterization of these ultrafine particles. Since mixing these particles is most challenging, all of the mixing methods/devices (solvent-based, supercritical CO_2 and dry-based) available in our laboratory were tested, so that a comparison of the mixing performance of these methods could be made. All of the available instruments were also used to characterize the nanomixtures obtained.

Characterization of MS-3 mixtures

In order to evaluate the performance of the various mixing methods, an unambiguous approach to characterizing the mixture must first be achieved. Therefore, a high-resolution FESEM (JEOL 6700F), AFM (DI Nanoscope IIIa), TEM (Philips CM20), EELS (VG Microscopes, HB501 UX STEM) and EELS (LEO 922 TEM with an Omega Filter), as well as EDS microanalysis (LEO 982 Digital FESEM equipped with an Oxford X-ray detector) were used to characterize MS-3 mixtures processed using different mixing systems.

Results of FESEM analysis. Figure 5 shows two SEM photographs at different magnification of the MS-3 mixtures processed using HYB at a rotation speed of 8k rpm. By using a state-of-the-art SEM (JEOL 6700F), extremely high magnification can be achieved, and therefore, primary particles can be clearly distinguished from each other. However, it was very difficult to identify individual silica or titania particles from the images since they do not possess different shape characteristics. The Degussa P25 is an anatase type TiO_2 while the R972 is a fumed silica (hence, amorphous (Sheka et al., 1999)). This suggests that the crystalline (cubic) particles in the images are more likely to be TiO_2 and the chain-like with round head particles (see arrow in Figure 5B) are probably SiO_2. The chain-like structure of silica is also observed in Figure 7 as discussed later. The BSE detector was also used to differentiate between the two kinds of particles. However, good results were not obtained probably because the BSE detector collects electrons that are elastically scattered from deeper surface layers (about 100 nm), which is much larger than the size of either of the two component particles, resulting in a blended signal of both elements. Moreover the difference in atomic number between Ti and Si is not high enough for the BSE detector to produce a noticeable difference in gray scale on the SEM images.

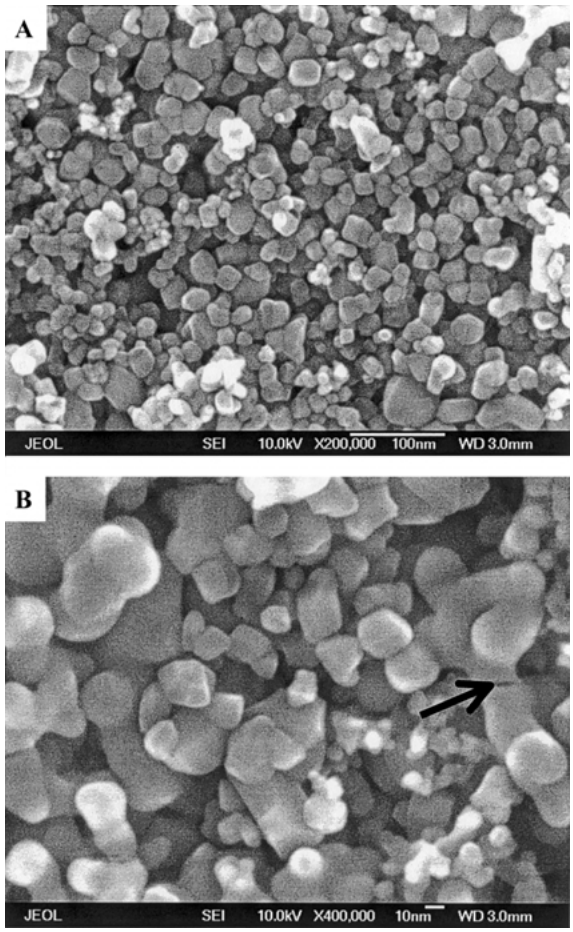

Figure 5. SEM micrographs of MS-3 mixture processed using HYB for 5 min at 8k rpm: (a) 200k×, (b) 400k×.

Results of AFM analysis. The AFM has been widely used in characterizing nanostructures since its invention (Friedbacher et al., 1991; Dai et al., 1995; Prica et al., 1998; Wittborn et al., 2000). The use of AFM in phase imaging (Sheehan & Lieber, 1993; Babcock & Prater, 1998), as discussed above, should make it possible to distinguish between different particles in a mixture. Therefore, the DI Nanoscope IIIa AFM was used to obtain topographical images of the MS-3 mixtures produced using RESS, the Hybridizer (HYB) and solvent-based methods. It is not difficult to 'see' the nanosized particles from an AFM measurement (see Figure 6, showing an AFM image of a solvent-based mixed sample, Hexane/30 min). However, the phase

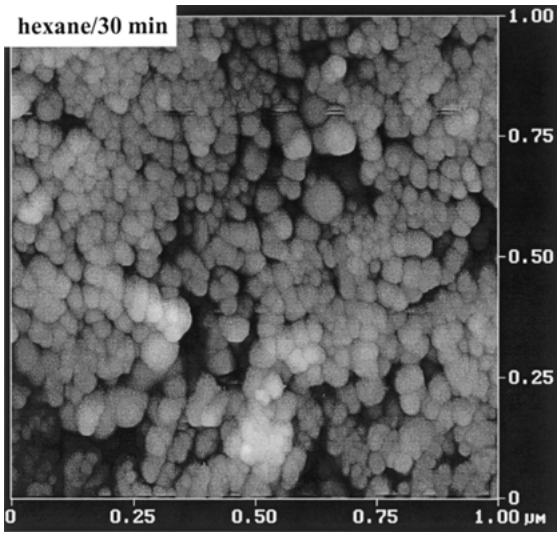

Figure 6. AFM micrograph of MS-3 mixture processed using hexane with ultrasonication for 30 min.

imaging mode could not differentiate SiO_2 from TiO_2 in the MS-3 mixtures. One possible reason is that the two materials may be too close in surface force properties. While these preliminary results are not very promising, more research is required to fully utilize the capabilities of the AFM for mixing characterization.

Results of high-resolution TEM analysis. TEM has been extensively used to characterize nanoparticles and structures because of its high resolution (Williams & Carter, 1996; Wang et al., 1997; Qiu et al., 2000). Figure 7 shows the TEM images of TiO_2, SiO_2 and the TiO_2/SiO_2 mixture obtained from HYB processing using the Philips CM20. It is seen that SiO_2 appears as chain-shaped aggregates while TiO_2 appears as crystalline particles. A hasty inspection of Figure 7(c) might indicate that the two powders have been well mixed, at least at a scale of a hundred nanometers, since we can see both particles next to one another or overlapping. However, the chained SiO_2 particles seen in the center of the image (see arrow) are clearly unmixed, although a very high rotation speed (16k rpm) was used in the processing. Because nanoparticles often tend to form chained aggregates and behave as a polymer (Friedlander, 1999), it is not easy to break them down into individual particles.

In principle, one can identify individual particles in the mixture by using electron diffraction. However, in general, a mixture sample under TEM would have overlapping of two species, hence it is difficult to identify individual particles in the mass of the mixture. This implies that direct TEM imaging is not very useful for any quantitative characterization of nanoparticle mixing; hence energy filtering may be a better alternative, and is considered next.

Results of EELS analysis. A unique advantage of EELS is energy filtering. It provides an ability to obtain a very high-resolution elemental map of the sample. Figure 8 shows an EELS image (done at Oak Ridge National Lab) of the MS-3 mixture processed using HYB, and the corresponding Ti and Si maps. The upper right image (c) in Figure 8 is a zero energy loss filtered image of an agglomerate of TiO_2/SiO_2 mixture. The Ti map over the agglomerate is shown in the left image (a) and the Si map in the lower right image (b). The bright particles/aggregates in the mapping images are the corresponding particles of TiO_2 or SiO_2. This is a remarkable result, indicating that a dry powder mechanical mixing device (HYB) can achieve mixing at the nanoscale.

Another MS-3 mixture sample processed in hexane for 30 min was measured using a LEO 922 TEM equipped with the Omega filter (EELS). The results are shown in Figure 9. Figure 9(a) shows the EELS spectra of Ti and Si in the mixture, (b) is a traditional TEM image of a group of mixed particles, and (c) is an energy filtering enhanced image of the same group of mixed particles.

It is clear from Figures 8 and 9 that EELS is able to distinguish TiO_2 and SiO_2 from their mixture, hence it has the capability of characterizing the mixing of nanoparticles at the nanoscale. However, it should be noted that unless many different samples of the mixture are imaged, one should not draw any conclusions regarding the total mixture quality.

Results of EDS spot analysis. An energy dispersive X-ray detector is usually available with an SEM. By analyzing a micro-area or spot of about 1 μm over a sample surface, a ratio of the two positive elements composing the two component particles can be obtained. A comparison of the atomic ratio of these elements obtained from random spots on a sample surface would be able to indicate a degree of homogeneity across the mixture sample. When enough data points are collected, a statistical analysis can also be done, that is, a standard deviation can be calculated. Thus, by comparing the standard deviation of the atomic ratio data obtained from different

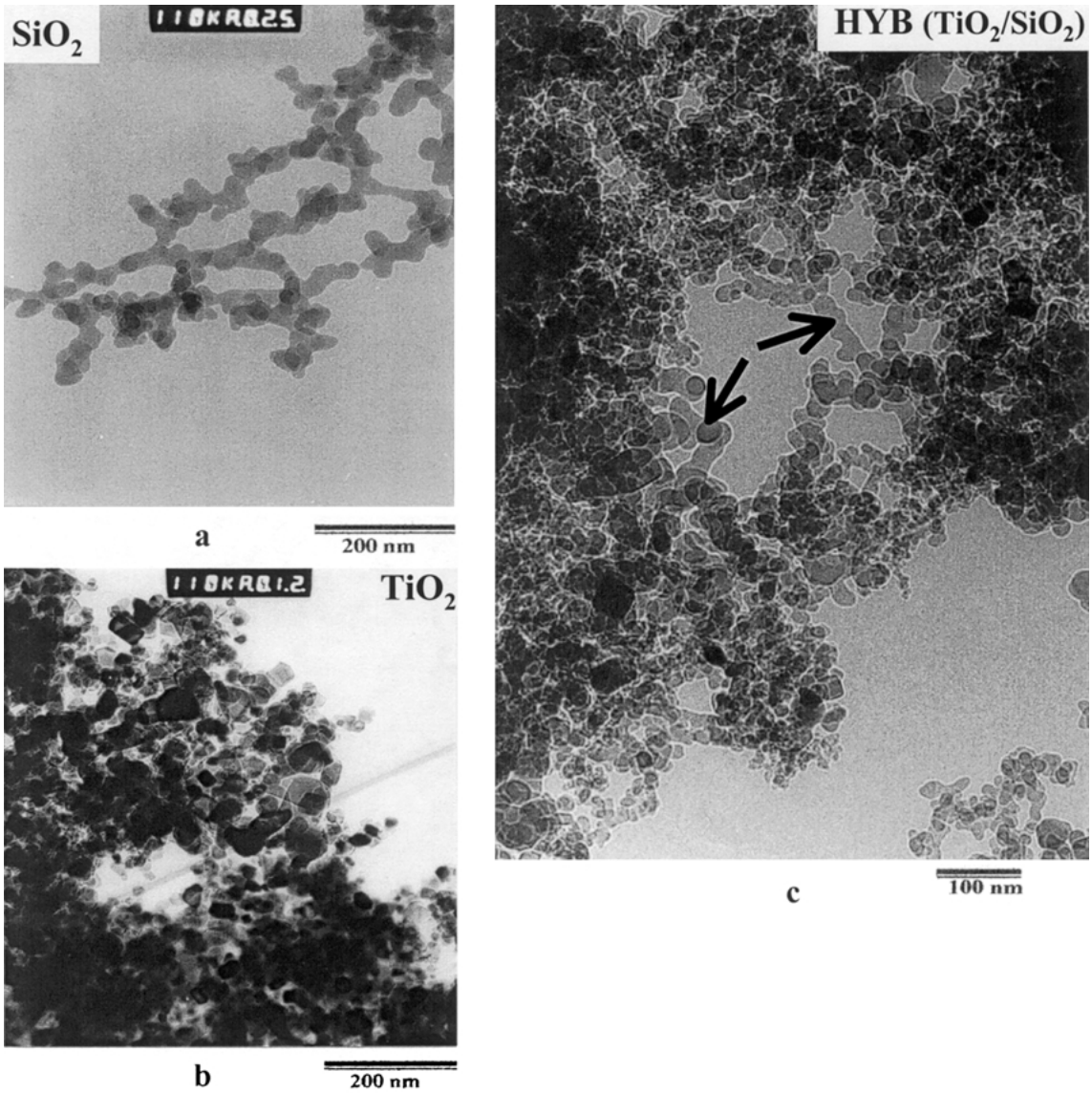

Figure 7. TEM micrographs of (a) SiO_2, (b) TiO_2 and (c) TiO_2/SiO_2 mixture (MS-3) processed using HYB at16k rpm for 5 min.

samples, it is possible to draw conclusions regarding the homogeneity or degree of mixing achieved in mixing of nanopowders. This approach is similar to the statistical methods described by (Fan et al., 1990; Rhodes, 1998; Weinekotter & Gericke, 2000) used for the characterization of free-flowing granular mixtures.

Figure 10 shows a typical spectrum obtained from one spot. Twenty randomly selected spots on a compressed wafer made from each of the processed MS-3 mixtures were analyzed. The atomic ratio of Ti/Si was calculated for all 20 random spots for each processing method and is listed in Table 2. A statistical analysis was performed for each group of data and the standard deviations are also listed in Table 2. The results are also illustrated in Figures 11 and 12.

An examination of Table 2 suggests that the Ti/Si ratio varies from spot to spot within each sample (columns in the table), and the variation differs with the processing method/conditions used for mixing as indicated by the standard deviation. The Ti/Si ratio data obtained for different processing methods in Table 2 were converted into frequency distribution plots and are

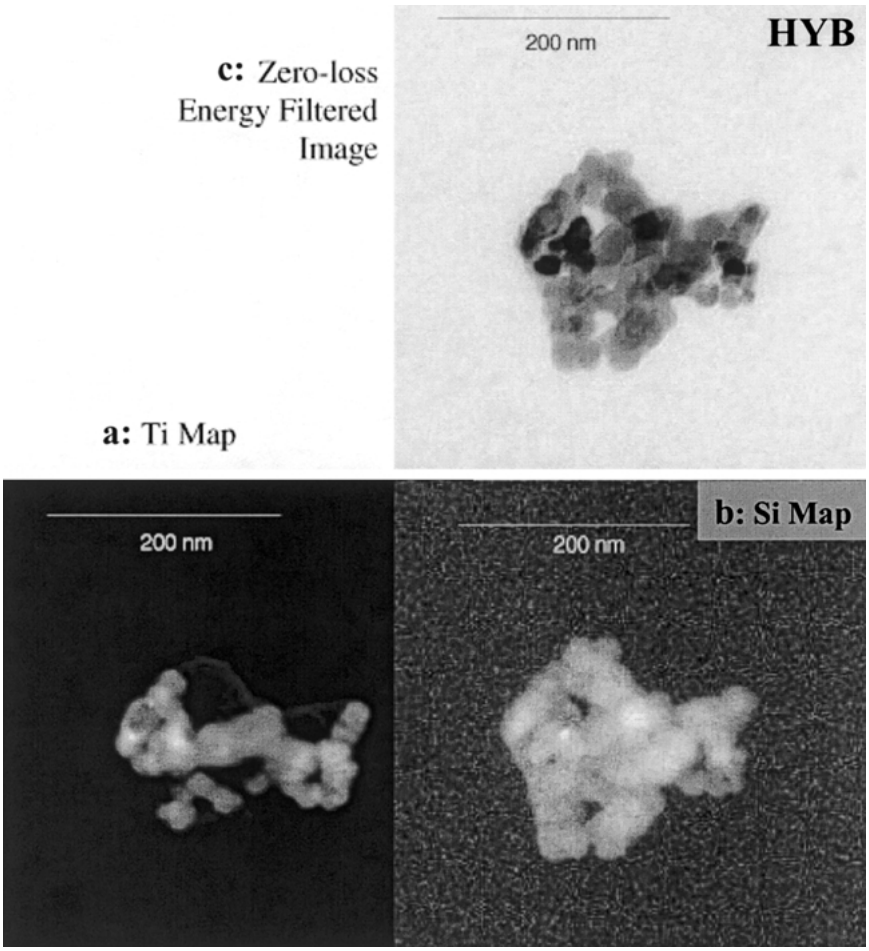

Figure 8. EELS micrographs of (c) an MS-3 mixture processed using HYB at 16k rpm for 5 min, and (a) Ti map, (b) Si map.

presented in Figures 11 and 12. In all of the frequency distribution plots, the expected mean value is 1.7, and an ideal mixture would exhibit a sharp peak around this mean. However, as seen in the figures, none of the mixing methods produced ideal results. Wet mixing based on EtOH, ultrasonicated for 30 min gives the best results, with RESS and the Hybridizer close behind.

The computed values of the standard deviation from Table 2 are also plotted in Figure 13. The figure shows that EtOH, ultrasonicated for 30 min, RESS and the Hybridizer show the lowest values for the standard deviation, corroborating the results shown in Figures 11 and 12.

It should be noted that while elemental microanalysis using EDS is a simple procedure, it cannot provide information down to the nanoscale since the interaction volume of the electron beam with the sample surface is about 1 μm^3 (depending on accelerating voltage, atomic number and the density of the material to be examined). In addition, the EDS analysis is not a very accurate quantitative technique; thus, the results need to be interpreted in conjunction with other more accurate characterization methods. Nevertheless, EDS microanalysis can provide quantitative results for the characterization of mixing of nanopowders, if a statistically meaningful numbers of data points are used.

Comparison of the performance of different mixing methods

In order to compare the performance of the methods/devices employed in this study, the experiments were designed so that each device is operated close to its maximum capability in terms of providing

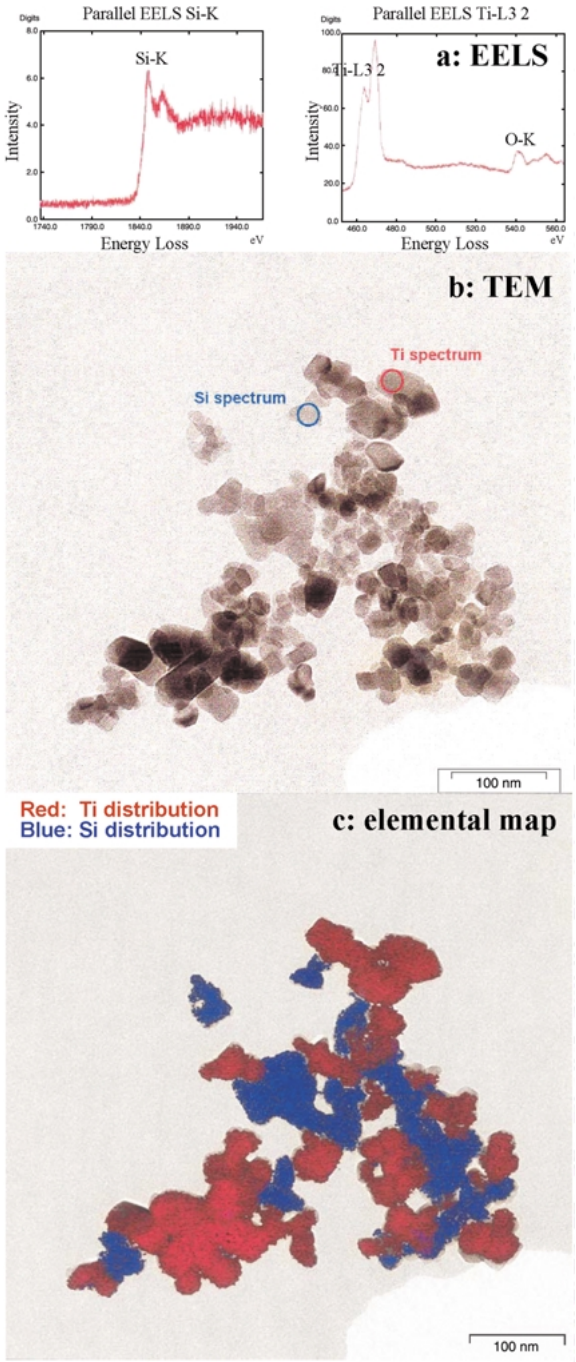

Figure 9. EELS results for an MS-3 mixture using hexane under ultrasonication for 30 min: (a) EELS spectra for Ti and Si, (b) TEM image of an agglomerate of the mixture, and (c) an energy-filtering enhanced image of the same agglomerate in (b).

kinetic energy for deagglomeration and sufficient processing time for mixing to occur. It should be noted, however, that for the RESS system, moderate operating conditions (P, T and rpm) were chosen. The resultant MS-3 mixtures were characterized as to their degree of mixing or homogeneity using the EDS microanalysis method as described above.

From Table 2 (standard deviation) and Figures 11–13, the performance of the various processing methods can be divided into two groups: (1) solvent-based, RESS and HYB, and (2) MF, MAIM and MIC. The methods in the first group performed generally better than the methods in the second group. However, within the first group, the RESS process and the hybridizer performed almost as good as the solvent-based methods.

The solvent-based methods are attractive, because the particles can be easily dispersed due to the low surface tension of EtOH and hexane. It should be noted, however, that good mixing results were not obtained by simple stirring the suspension of MS-3 in either of the two solvents used. Hence it is clear that ultrasonic agitation is necessary to enhance the dispersion (breakup of agglomerates) and mixing. The mechanism of ultrasonic agitation is based on acoustic cavitation in a liquid phase, that is, the formation, growth and impulsive collapse of bubbles in the liquid phase. Cavitation serves as a means of concentrating the diffusive energy of sound (Suslick, 1990; 1995). The bubble collapse produces intense local heating (temperatures of roughly 5000 K), high pressures (about 1700 atm) and very short lifetimes (a duration of 100 ns) (Suslick et al., 1986; Suslick, 1995). In short, the degree of agitation produced by ultrasonic cavitation in a liquid phase is extremely high. Hence, it is not difficult to explain the much better mixing performance obtained with solvent-based methods when coupled with ultrasonic agitation.

However, a comparison between the results using EtOH and hexane implies that the type of solvent also plays a role in the dispersion of the component powders since ethanol performed better than hexane. A possible explanation can be derived from the polarity of the two types of solvent molecules. Hexane is non-polar and hydrophobic while ethanol is polar and hydrophilic. Both powders used in the experiments had a small amount of water content (approximately 0.5% for SiO_2 and 1.2% for TiO_2). The adsorbed water might have formed a layer/layers over the surface of the primary particles, which can greatly enhance the interparticle forces within an agglomerate. Therefore, hydrophilic

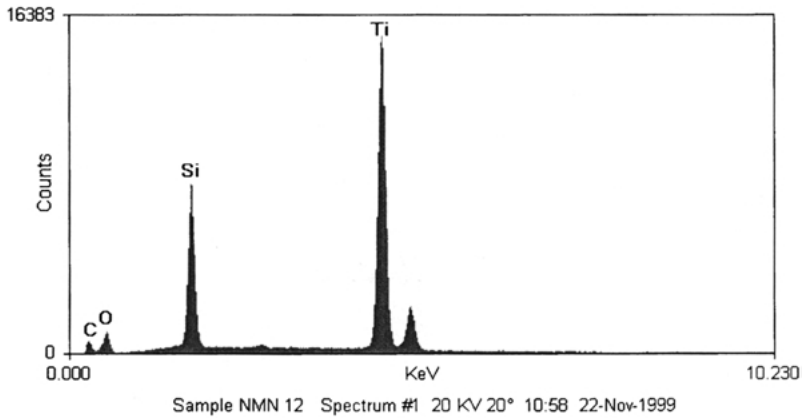

Figure 10. EDS spectrum of an MS-3 mixture processed in EtOH under ultrasonic agitation for 5 min.

Table 2. Summary of EDS elemental analysis (Ti/Si ratio) on randomly selected spots on the sample surface for different methods/conditions, SD is the standard deviation

Method	Ti/Si atomic ratio (X_i)								
	MF	HYB	MIC	MAIM	RESS	EtOH (5 min)	EtOH (30 min)	Hexane (5 min)	Hexane (30 min)
1	1.56	1.80	1.31	1.42	1.60	2.36	1.62	1.27	1.46
2	2.04	1.43	1.10	2.99	1.27	2.18	1.68	2.11	1.15
3	1.66	1.97	3.11	0.92	1.61	1.48	2.01	1.37	1.34
4	1.29	0.92	1.27	1.48	1.77	1.90	1.67	1.67	2.65
5	2.34	1.81	2.39	2.28	1.56	1.77	1.68	1.63	1.35
6	1.68	1.89	3.05	1.30	2.11	1.11	1.57	2.29	1.76
7	2.75	1.72	1.05	2.41	1.81	1.41	1.84	1.65	1.28
8	1.52	2.12	1.22	0.96	1.95	1.78	1.62	2.11	1.78
9	1.44	1.65	1.39	1.82	2.14	1.34	2.22	2.43	2.35
10	1.56	1.56	3.41	2.28	1.81	2.00	1.61	1.96	2.14
11	2.04	1.22	0.42	1.68	1.47	2.10	1.74	2.02	1.64
12	1.66	1.81	0.81	2.21	2.19	1.95	1.76	1.25	1.35
13	2.79	2.39	3.51	1.06	1.66	1.47	1.74	1.10	1.69
14	1.52	1.54	1.27	1.89	1.38	1.70	1.59	1.90	1.33
15	1.38	1.73	2.69	2.79	2.01	2.13	1.36	2.68	1.59
16	2.36	1.27	2.21	2.17	1.84	1.96	1.58	1.12	1.99
17	1.16	1.62	0.52	1.22	1.57	1.70	2.11	2.34	1.66
18	1.09	1.92	1.25	2.49	1.41	1.43	1.87	1.42	1.41
19	2.14	1.65	3.22	0.92	2.37	1.40	1.75	1.91	1.78
20	1.48	1.18	0.69	1.28	1.91	1.61	1.67	1.16	1.57
X_{ave}	1.77	1.67	1.80	1.78	1.77	1.74	1.73	1.77	1.66
SD	0.48	0.33	1.01	0.63	0.29	0.32	0.20	0.46	0.39

ethanol should be able to penetrate through the inter-particle spaces much easier than hydrophobic hexane. One might argue that the high temperature produced by bubble collapse could have heated the agglomerate and gasified the adsorbed water. This may not occur, however, since the frequency of ultrasound used in the experiment is 44 kHz, with an equivalent wavelength slightly larger that 20 μm. Thus, the ultrasonic wave would not significantly affect the agglomerates (usually smaller than 1 μm). This could have made the ultrasonic cavitation more like agitation than heating.

Table 2 and Figure 13 also show that the mixing performance of RESS is generally better than that of the dry methods, and comparable to the solvent-based methods. The idea behind the RESS process is to

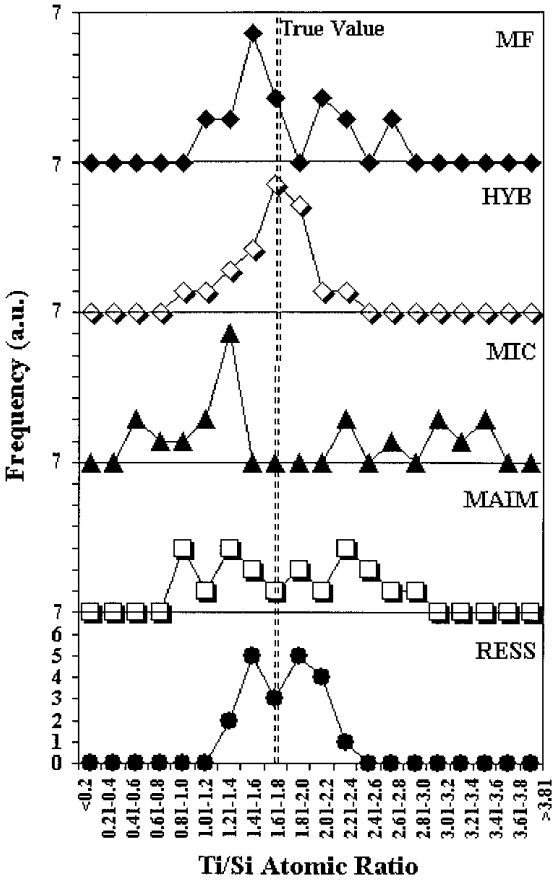

Figure 11. Plots of frequency against Ti/Si ratio interval obtained from EDS elemental analysis on MS-3 mixtures processed using various methods: MF (2k rpm, 30 min), HYB (16k rpm, 5 min), MIC (1.2k rpm, 5 min), MAIM (30 min) and RESS (135 atm, 46°C, 1500 rpm).

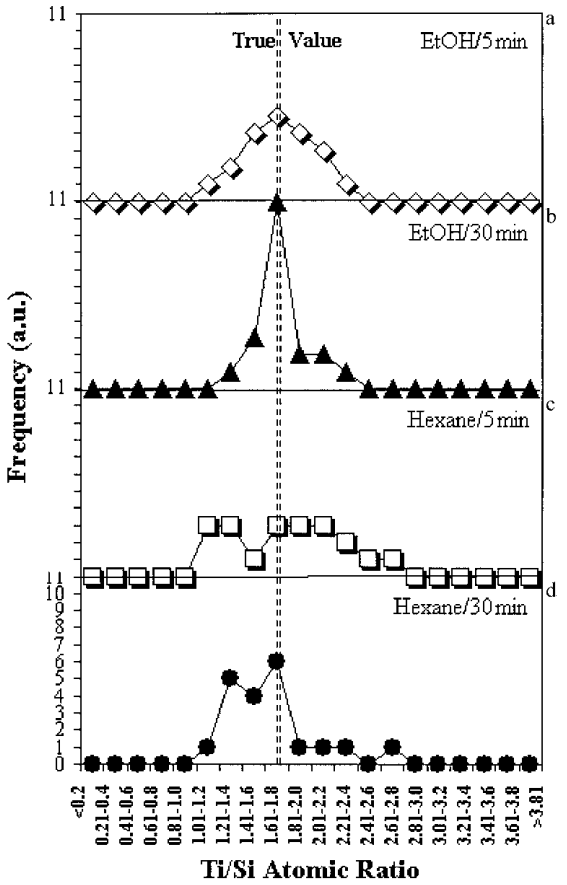

Figure 12. Plots of frequency against Ti/Si ratio interval obtained from EDS elemental analysis on MS-3 mixtures processed using solvent-based methods: (a) EtOH: ultrasonic agitation for 5 and (b) 30 min, and (c) hexane: ultrasonic agitation for 5 and (d) 30 min.

utilize the extremely low viscosity of supercritical CO_2 (i.e., very high permeability) so that the interparticle voids within an agglomerate can be filled up with CO_2. When the supercritical suspension is released through a nozzle, the rapid depressurization causes the rate of CO_2 vaporization to be much faster than the rate of diffusion of CO_2 through the micro porous network within the agglomerate. As a result, an 'explosion' would occur in the agglomerates in the receiving tank (see Figure 1) and homogeneous mixing can be achieved. This idea is illustrated schematically in Figure 14(a).

RESS has been used for many applications (Alessi et al., 1996; Turk, 1999; York, 1999) other than mixing of nanopowders. Three major parameters can affect the performance of the RESS system in terms of mixing: pressure, temperature and stirring speed. Pressure essentially determines the permeability of CO_2, and more importantly the driving force for the 'explosion' of an agglomerate. Temperature affects the permeability of CO_2 and also has a possible impact on removing adsorbed water, which plays an important role in keeping the primary particles agglomerated. Stirring keeps the powders suspended and may affect the homogeneity of the final mixture as well. In this study, the full capability of our supercritical CO_2 system (500 atm, 350°C and stirring at 2500 rpm) has not been utilized. It is therefore suggested that the RESS system be systematically studied in order to determine the optimum operating parameters to achieve homogeneous mixing of nanopowders.

The performance of the dry mixing devices varies greatly from one to another, as shown in Table 2 and

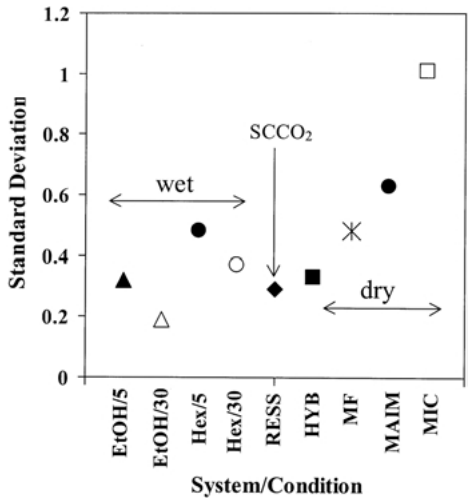

Figure 13. Standard deviation of data of Ti/Si ratio obtained from EDS elemental analysis from MS-3 mixtures processed using different methods or under different conditions.

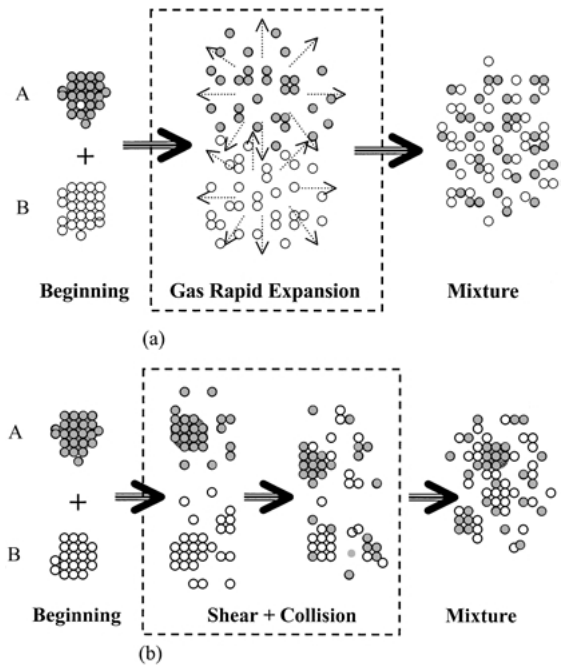

Figure 14. Schematic representations of the possible mixing mechanisms for different mixing processes: (a) RESS and (b) high-energy mechanical dry processing systems.

Figures 11–13. The major forces in the dry mechanical devices for breaking up agglomerates are compressive, shear and impaction forces. These forces provide sufficient energy for the agglomerates to be either crushed, or have their corners, edges and outer surfaces removed as well as undergoing repeated collisions with each other as illustrated schematically in Figure 14(b). This mutual exchange of particles within the agglomerates should result in good mixing.

Each of these dry mechanical devices, while having much in common as a group, has unique features with regards to providing forces of different types and intensities. From the design of a device, and the flow patterns of the particles inside the device and its power consumption, it is possible to predict its performance as a mixer. In terms of both energy consumption and the kinetic energy provided under the operating conditions used in our experiments, the devices can be rated in decreasing order as HYB, MF, MIC and MAIM.

Therefore, it is not difficult to understand that the HYB showed the best mixing performance when high-energy collisions between particles and the blades (including the circulation tube) are achieved at a rotation speed of 16k rpm (Honda et al., 1988; 1994; Ishizaka et al., 1993). However, it is surprising that the HYB is competitive with both the solvent-based methods and the RESS process.

Although MIC is considered a high-intensity machine as compared to the MAIM, MAIM seems to have performed better than MIC (see Table 2 and Figures 11–13). This is probably due to the fact that the MIC was used here under dry conditions, while it is designed for grinding materials in liquid suspension (Hamada & Senna, 1995; 1996). The large gap between the rotating rings and the bottom of the vessel might act as dead space, where dry powder can accumulate due to gravity, resulting in a poorer degree of mixing, whereas this would probably not occur in a liquid suspension.

Summary

Methods for mixing and characterizing the degree of mixing of nanopowders have been presented. Novel mixing techniques such as the RESS and high-intensity mechanical-based dry powder processing are proposed as an alternative to environmentally unfriendly solvent-based mixing methods. It is shown that at least one of the dry powder processing methods, the Hybridizer, and the RESS process perform nearly as well as the solvent-based methods in terms of producing a homogeneous mixture of nanopowders.

For the characterization of nanopowder mixtures, a number of conclusions can be drawn. For powder mixtures with very distinct shape characteristics

(like W and MoO_3), high-resolution FESEM is suitable for characterizing the degree of mixing. The BSE detector is found to be capable of distinguishing between different particles of similar shape having different chemical composition if the difference in atomic number between the two positive elements is sufficiently large (e.g., W and Ti). For nanoparticles, which do not possess these characteristics such as TiO_2/SiO_2, characterization is much more difficult. FESEM, AFM and TEM can characterize the mixtures to a certain extent, but are generally insufficient by themselves, and further study is recommended to make them more useful. EELS, however, is capable of distinguishing between two nanoparticles such as TiO_2 and SiO_2 in a mixture but is not readily available. Finally, EDS spot analysis can be easily used to characterize mixtures of TiO_2 and SiO_2 if enough spots (data points) are collected and a statistical analysis is applied. This appears to be the most convenient technique for generating quantitative results, albeit at the micron scale.

Acknowledgements

The authors would like to thank the US Army, Picatinny Arsenal for financial support through contract # DAAE30-98-C-1050, the National Science Foundation for financial support through grant # CTS-9985618, and the New Jersey Commission of Science and Technology for financial support through contract # 01-2042-007-24. The authors are also grateful to Prof. M. Libera of Stevens Institute of Technology for his assistance in using TEM and EELS and the many valuable discussions with him to help interpret the results obtained. Thanks are also due to Dr. James Bentley of Oak Ridge National Laboratory and the staff of LEO, USA for their help with the energy-filtered imaging results. Dr. Bentley's research at the Oak Ridge National Laboratory, SHaRE Collaborative Research Center was sponsored by the Division of Materials Sciences and Engineering, US Department of Energy, under contract DE-AC05-00OR22725 with UT-Battelle, LLC, and through the SHaRE Program under contract DE-AC05-76OR00033 with Oak Ridge Associated Universities.

References

Ajayan P.M., 1995. Carbon nanotubes and nanocomposites. Fullerene Sci. Technol. 3(3), 119.

Ajayan P.M., Ph. Redlich & M. Rule, 1997. Structure of carbon nanotube based nanocomposites. J. Microscopy 185, 275.

Alessi P., A. Cortesi, I. Kikic, N.R. Forster, S.J. Macnaughton & I. Colombo, 1996. Particle production of steroid drugs using supercritical processing. Ind. Eng. Chem. Res. 35, 4718–4726.

Babcock K.L. & C.B. Prater, 1998. Phase Imaging: Beyond Topography. Digital Instruments, Inc., Rev. 4.

Brone D. & F.J. Muzzio, 1998. Enhanced mixing in double-cone blenders. Powder Technol. 110(3), 179–189.

Brone D., A. Alexander & F.J. Muzzio, 1998. Quantitative characterization of mixing of dry powder in V-blenders. AIChE J. 44, 271–278.

Carter S.A., J.C. Scott & P.J. Broack, 1997. Enhanced luminance in polymer composite light emitting device. Appl. Phys. Lett. 71, 1145–1147.

Chen J., H. Herman & C.C. Huang, 1997. A preliminary model for mechanofusion powder processing. KONA 15, 113–120.

Dai H., E.W. Wong, Y.Z. Lu, S. Fan & C.M. Lieber, 1995. Synthesis and characterization of carbide nanorods. Nature 375, 769.

Danckwerts P.V., 1953. Theory of mixture and mixing. Research 6, 355–361.

Endo Y., Sh. Hasebe & Y. Kousaka, 1997. Dispargation of aggregates of the powder by acceleration in an air stream and its application to the evaluation of adhesion between particles. Powder Technol. 91, 25–30.

Fan L.T., Y.M. Chen & F.S. Lai, 1990. Recent development in solids mixing. Powder Technol. 61, 255–278.

Fokema M.D., A.J. Zarur & J.Y. Ying, 2000. Lean-Burn natural gas engine exhaust remediation using nanostructured catalysts and coatings. In: Chow G.-M., Ovid'ko I.A. and Tsakalakos T. eds. Nanostructured Films and Coatings. Kluwer, Dordrecht, the Netherlands, pp. 355–365.

Friedbacher G., P.K. Hansma, E. Ramli & G.D. Stucky, 1991. Imaging powders with the atomic force microscope: From biominerals to commercial materials. Science 253, 1261–1263.

Friedlander S.K., 1999. Polymer-like behavior of inorganic nanoparticle chain aggregates. J. Nanoparticle Res. 1, 9–15.

Goldstein J.I., D.E. Newbury, P. Echlin & D.C. Joy, 1992. Scanning Electron Microscopy and X-Ray Microanalysis: A Text for Biologists, Materials Scientists, and Geologists. 2nd edn., pp. 189–230.

Gross K.J., P. Spatz, A. Zuttel & L. Schlapbach, 1996. Mechanically milled Mg composites for hydrogen storage: the transition to a steady-state composition. J. Alloys and Compounds 240, 206–213.

Gulliver E., R.E. Riman & V.A. Greenhut, 1997. Mixedness engineering for advanced multicomponent materials. Int. J. Powder Metallurgy 33, 29–36.

Hamada K. & M. Senna, 1995. Kagaku Kogaku Ronbunshu 21, 334.

Hamada K. & M. Senna, 1996. Mechanochemical effects on the properties of starting mixtures for $PbTiO_3$ ceramics by using a novel grinding equipment. J. Mater. Sci. 31, 1925–1928.

Harnby N., 1978. Statistics as an aid to powder mixing. International Symposium on Mixing, Faculte Polytechnique de Mons, Feb. 21–25, paper D3.

Hendrickson W.A. & J. Abbott, 1999. US Patent: 5962082.

Hill K.M., J.F. Gilchrist, J.M. Ottino, D.V. Khakhar & J.J. McCarthy, 1999. Mixing of granular materials: a test-bed dynamical system for pattern formation. Int. J. Bifur. Chaos 9(8), 1467–1484.

Honda H., M. Kimura, F. Honda, T. Matsuno & M. Koishi, 1994. Preparation of monolayer coated powder by dry impact blending process utilizing mechanochemical treatment. Colloids Surf. A: Physicochem. Eng. Aspects 82, 117–128.

Honda H., T. Matsuno & M. Koishi, 1988. J. Soc. Powder Technol. Jpn. 25, 597.

Imanaka N., J. Kohler & M. Toshiyuki, 2000. Inclusions of nanometer-sized Al_2O_3 particles in a crystalline $(Sc,Lu)_2(WO_4)_3$ matrix. J. Am. Ceram. Soc. 83, 427–429.

Ishizaka T., H. Honda & M. Koishi, 1993. Drug dissolution from indomethacin-starch hybrid powders prepared by dry blending method. J. Pharm. Pharmacol. 45, 770–774.

Kaye B.H., 1997. Powder Mixing. Chapman & Hall, pp. 19–35, 77–131.

Kear B.H. & G. Skandan, 1997. Nanostructured bulk materials: synthesis, processing, properties and performance. In: Seigel R.W., Hu E. and Reco M.C. eds. Proceedings of R&D Trends in Nanoparticles, Nanostructured Materials and Nanodevices in the United States, pp. 103–117.

Kear B.H. & G. Skandan, 1999. Overview: status and current developments in nanomaterials. Int. J. Powder Metallurgy 35(7), 35–37.

Koishi M., H. Honda, T. Ishizaka, T. Matsuno, T. Katano & K. Ono, 1987. Chimicaoggi 5, 43.

Kristensen H.G., 1996. Particle agglomeration in high shear mixer. Powder Technol. 88, 197–202.

Kwak S.Y., 1994. Determination of microphase structure and scale of mixing in poly-epsilon-caprolactone (PCL)/poly (vinylchloride) (PVC) blend by high-resolution solid-state 13C-NMR spectroscopy with magic angle spinning and cross polarization. J. Appl. Polym. Sci. 53(13), 1823–1832.

Lacey P.M.C., 1954. Developments in the theory of particulate mixing. J. Appl. Chem. 4, 257.

Maser W.K., I. Lukyanchuk, P. Bernier, P. Molini, S. Lefrant, Ph. Redlich & P.M. Ajayan, 1997. Superconducting RNi_2B_2C (R = Y, Lu) nanoparticles: size effects and weak links. Adv. Mater. 9, 503.

Moser W.R., J.E. Sunstrom IV & B. MarshikGuerts, 1996. The synthesis of nanostructured pure phase catalysts by hydrodynamic cavitation. In: Moser W.R. ed. Advanced Catalysts and Nanostructured Materials. Academic Press, pp. 285–305.

Myers D., 1999. Surfaces, Interfaces, and Colloids: Principles and Applications. 2nd edn. Wiley-VCH, pp. 40–67.

Myers K.J., M.F. Reeder, D. Ryan & G. Daly, 1999. Get a fix on high-shear mixing. Chem. Eng. Prog. Nov. 1999, pp. 33–42.

Ottino J.M. & D.V. Khakhar, 2000. Mixing and segregation of granular materials. Annu. Rev. Fluid Mech. 32, 55–91.

Parent J.O.G., J. Iyengar & H. Henein, 1993. Fundamentals of dry powder blending for metal matrix composites. Int. J. Powder Metallurgy 29, 353–366.

Pfeffer R., R. Dave, D. Wei & M. Ramlakhan, 2001. Synthesis of engineered particulates with tailed properties using dry particle coating. Powder Technol. 117, 40–67.

Pierre A.C., 1998. Introduction to Sol-Gel Processing. In: Lisa Klein ed. The Kluwer International Series in Sol-Gel Processing: Technology and Applications. Kluwer Academic Publishers, Boston/Dordrecht/London, pp. 220–247.

Poux M., P. Fayolle, J. Bertrand, D. Bridoux & J. Bousquet, 1991. Powder mixing: some practical rules applied to agitated systems. Powder Technol. 68(3), 213–234.

Prica M., K. Kendall & S.A. Markland, 1998. Atomic force microscope study of ceramic powder compacts during drying. J. Am. Ceram. Soc. 81(3), 541–548.

Qiu S., J. Dong & G. Chen, 2000. Synthesis of CeF_3 nanoparticles from water-in-oil microemulsions. Powder Technol. 113, 9–13.

Ramlakhan M., C.-Y. Wu, S. Watano, R.N. Dave & R. Pfeffer, 2000. Dry particle coating using magnetically assisted impaction coating (MAIC): modification of surface properties and optimization of system and operating parameters. Powder Technol. 112, 137–148.

Reverchon E, G. Donsi & D. Gorgoglione, 1993. Salicylic acid solubilization in supercritical CO_2 and its micronization by RESS. J. Supercrit. Fluids 6(4), 241–248.

Rhodes M., 1998. Introduction to Particle Technology. John Willey & Sons, West Sussex, England, pp. 223–235.

Roco M.C., 1999. Nanoparticles and nanotechnology research. J. Nanoparticle Res. 1(1), 1–6.

Rumpf H., 1962. In: Krepper W.A. ed. Agglomeration. Wiley, New York, p. 379.

Sheehan P.E. & C.M. Lieber, 1996. Nanotribology and nanofabrication of MoO_3 structures by atomic force microscopy. Science 272, 1158–1161.

Sheka E., V. Khavryutchenko & E. Nikitina, 1999. From molecules to particles: quantum-chemical view applied to fumed silica. J. Nanoparticle Res. 1, 71–81.

Siegel R.W., 1999. In: Siegel R.W., Hu E. and Reco M.C. eds. Nanostructure Science and Technology: A Worldwide Study. WTEC, Loyola College in Maryland, pp. 1–14.

Singh R.K., A. Ata, J. Fitz-Gerald & W. Hendrickson, 1997. Dry coating method for surface modification of particulates. In: Sudarshan T.S., Khor K.A. and Jeandin M. eds. Surface Modification Technology X. The Institute of Materials, London.

Suslick K.S., 1990. Sonochemistry. Science 247, 1439–1445.

Suslick K.S., 1995. Applications of ultrasound to materials chemistry. MRS Bulletin, April, pp. 29–34.

Suslick K.S., D.A. Hammerton & R.E. Cline Jr., 1986. The sonochemistry hot spot. J. Am. Chem. Soc. 108, 5641.

Tanno K., T. Onagi & M. Naito, 1994. Preparation of steel/zirconia composite particles with a multiphase coating layer. Adv. Powder Technol. 5(4), 393–405.

Thiel W.J. & P.L. Stephenson, 1982. Assessing the homogeneity of an ordered mixture. Powder Technol. 31, 45–50.

Tom J.W. & P.G. Debenedetti, 1991. Formation of bioerodiable polymeric microspheres and microparticles by rapid expansion of supercritical solutions. Biotechnol. Prog. 7, 403–411.

Tom J.W., X. Kwauk, S.-D. Yeo & P.G. Debenedetti, 1993. Rapid expansion of supercritical solutions (RESS): fundamentals and applications. Fluid Phase Equil. 82, 311.

Trudeau M.L. & J.Y. Ying, 1996. Nanocrystalline materials in catalysis and electrocatalysis: structure tailoring and surface reactivity. Nanostr. Mater. 7(1/2), 245–258.

Turk M., 1999. Formation of small organic particles by RESS: experimental and theoretical investigations. J. Supercrit. Fluids 15, 79–89.

Verkhovluyk T.V., 1993. Determination of homogeneity of some composite materials. Ukrain. Khimi. Zh. 59, 3.

Wang R.H. & L.T. Fan, 1976. Ind. Eng. Chem. Process Dev. 15, 381.

Wang Y.C., T.M. Chou & M. Libera, 1997. Transmission electron holography of silicon nanosphere with surface oxide layers. Appl. Phys. Lett. 70(10), 1296–1298.

Weinekotter R. & H. Gericke, 2000. Mixing of Solids. Kluwer Academic Publishers, Dordrecht, the Netherlands, pp. 15–34.

Williams, D.B. & C.B. Carter, 1996. Transmission Electron Microscopy: A Textbook for Materials Science. Vol. 3, Plenum Press, New York.

Williams J.C., 1990. Mixing and segregation in powders. In: Rhodes M. ed. Principles of Powders Technology. John Wiley & Sons, Chichester, p. 71.

Wittborn J., K, Rao & J. Nogues, 2000. Magnetic domain and domain-wall imaging of sub-micron Co dots by probing the magnetostrictive response using atomic force microscopy. Appl. Phys. Lett. 76(20), 2931–2933.

Ying J.Y., 1997. Nanoparticle synthesis for catalytic applications. In: Proceedings of the Joint National Science Foundation-National Institute of Standards and Technology Conference on 'Nanoparticles: Synthesis, Processing into Functional Nanostructures, and Characterization'. National Science Foundation, Arlington, Virginia, pp. 131–137.

Yokoyama T., K. Urayama, M. Naito, M. Kato & T. Yokoyama, 1987. The angmill mechanofusion system and its applications. KONA 5, 59–67.

York P., 1999. Strategies for particle design using supercritical fluid technologies. Pharmaceut. Sci. Technol. Today 2, 430–440.

Zhang Z., C.-C. Wang, R. Zakaria & J.Y. Ying, 1998. Role of particle size in nanocrystalline TiO_2-based photocatalysts. J. Phys. Chem. B 102(52), 10871–10878.